33RD CONGRESS
OF THE INTERNATIONAL COUNCIL
OF THE AERONAUTICAL SCIENCES
STOCKHOLM, SWEDEN, 4-9 SEPTEMBER, 2022

ICAS 2022 SWEDEN

IMPACT OF MOTION–DEPENDENT ERRORS ON THE ACCURACY OF AN UNAIDED STRAPDOWN INERTIAL NAVIGATION SYSTEM

Krystian Borodacz[1] & Cezary Szczepański[2]

[1,2]Łukasiewicz Research Network – Institute of Aviation

Abstract

The selection of an appropriate measurement system for an inertial navigation system requires an analysis of the impact of sensor errors on the position and orientation determination accuracy to ensure that the selected solution is cost effective and complies with the requirements. In the solutions reported in the literature, this problem is solved based on the navigation duration only, by considering the time-dependent errors due to sensors bias and random walk parameters, or by simulation. In the former case, oversimplifying the analysis will not allow accurate values to be determined, while the latter method does not provide direct insight into the emerging dependencies. The article presents the results of the analysis carried out in an analytic way. General formulas are presented, which are also written in detail for the adopted model of the measurement system and various maneuvers. Although general equations are complicated, piece–wise constant motion variables were adopted, which allowed to distinguish fragments of equations, corresponding to individual error sources, which were discussed in the article. Presented formulas make evident and allow to understand dependencies occurring between motion parameters and navigation errors emerging as a consequence of maneuvers.

Keywords: INS, IMU, sensors, model, analysis

1. Introduction

Inertial navigation systems provide continuous localization even in case of outage or failure of other navigational means. However, the influence of measurement system errors results in a position determination error that increases with time and distance traveled. On the other hand, as the accuracy of sensors increases, their price also increases very rapidly. Thus, it is necessary to select an appropriate measurement system that provides a cost-effective solution and at the same time of sufficient accuracy, as it may determine the success of the mission. For this purpose it is necessary to analyze thoroughly how the measurement errors of the considered inertial measurement unit will influence the accuracy of the position determination.

As a first step, a coarse estimate of the required sensors accuracy can be determined based on the navigation duration only, by considering the time–dependent errors due to sensors bias and random walk parameters [2]. A more detailed analysis, however, requires consideration of errors that build up during motion due to the predicted trajectory and sensors sensitivity to motion parameters.

However, to the authors' knowledge and according to the literature review, there is a deficiency of such detailed analysis of this problem in the literature. In the analyses found, only the biases of the gyroscopes and accelerometers are considered, and for the more complicated cases that consider the influence of motion-dependent errors, only graphs for specific simulation or test cases are presented, without deriving detailed formulas. Nevertheless, the motion-dependent errors turn out to be significant, and the resulting effects, intriguing.

Article [8] presents results of an experimental study of a rotating inertial navigation system, showing that the introduction of system rotation can significantly reduce navigation errors. Indeed, the method of reducing navigational errors by setting the system into continuous rotation is generally known as 'carouseling' [7]. In contrast, [10] points out that in a practical implementation of rotating system,

additional orientation determination errors may arise. Analytical analysis of the navigational systems accuracy is performed in [1], where the reduction of position determination errors as a result of navigation system rotation is analytically presented. However, considerations are again limited to the errors of accelerometers and gyroscopes. A more complex model of the measurement system is presented by [12], although the model is used not to analyze the accuracy of the navigation system, but to calibrate the measurement system.
The paper will present the results of calculations of errors of orientation and position determination by an inertial navigation system. Calculations will be carried out for selected, different maneuvers and the assumed model of the measuring system. The emerging relationships will be analyzed and discussed. In the next section, the navigation and measurement system models used for the analysis will be described, and navigation error propagation formulas will be presented. Section 3 describes the methodology used and the maneuver cases considered. Detailed parameters of the measurement system are also presented. In Section 4 the obtained results are presented along with a discussion. The latest section contains conclusions.

2. General models

Accuracy analysis will be performed using basic unaided inertial navigation system (INS), presented in Figure 1, with the assumption of navigation coordinate system being inertial and orthogonal (flat-earth approximation). The measurement system is an inertial measurement unit (IMU), consisting of triad of orthogonal gyroscopes and triad of orthogonal accelerometers, whose outputs are measured values of specific force and body angular rate expressed in body coordinate system.

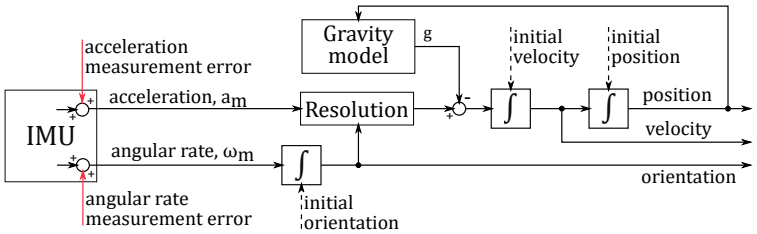

Figure 1 – Block diagram of basic strap-down INS

The values measured by the sensors include a measurement error described by an error model. The adopted model, presented in Equations (1) and (2), was developed based on information contained in standards, [4],[5],[6], and literature, [9],[13], whereby the effect of environmental conditions was neglected. In all of the following equations, the rule is that vectors are written in bold, while matrices in capital letters.

$$\boldsymbol{\omega_e}(t) = (S_\omega M_\omega - I)\,\boldsymbol{\omega}(t) + \boldsymbol{\omega_b} + \Omega_g M_\omega \boldsymbol{f_b}(t) + n_\omega \tag{1}$$

$$\boldsymbol{a_e}(t) = (S_a M_a - I)\,\boldsymbol{f_b}(t) + \boldsymbol{a_b} + n_a \tag{2}$$

where
$\boldsymbol{\omega_b}$, $\boldsymbol{a_b}$ — vector of measurement bias, for gyroscopes and accelerometers;
S_ω, S_a — matrix of sensitivity, for gyroscopes and accelerometers;
M_ω, M_a — matrix of input axes misalignment, for gyroscopes and accelerometers;
Ω_g — matrix of gyroscopes sensitivity to acceleration;
n_ω, n_a — gyroscopes and accelerometers measurement noise.
In addition to measurement errors, the navigation system also suffers from errors in determining initial conditions, and resulting errors in determining navigation parameters. However, an accurate knowledge of the gravity vector is assumed. A block diagram of the navigation system under consideration with the used symbols is shown in Figure 2. The symbols presented in the Figure 2, are:
$\boldsymbol{p}(t)$, $\boldsymbol{p_e}(t)$ — position in navigation coordinate system and error of its determination;
$\boldsymbol{v}(t)$, $\boldsymbol{v_e}(t)$ — velocity in navigation coordinate system and error of its determination;
$\boldsymbol{\alpha}(t)$, $\boldsymbol{\alpha_e}(t)$ — vector of rotation from navigation coordinate system to body coordinate system and error of its determination;

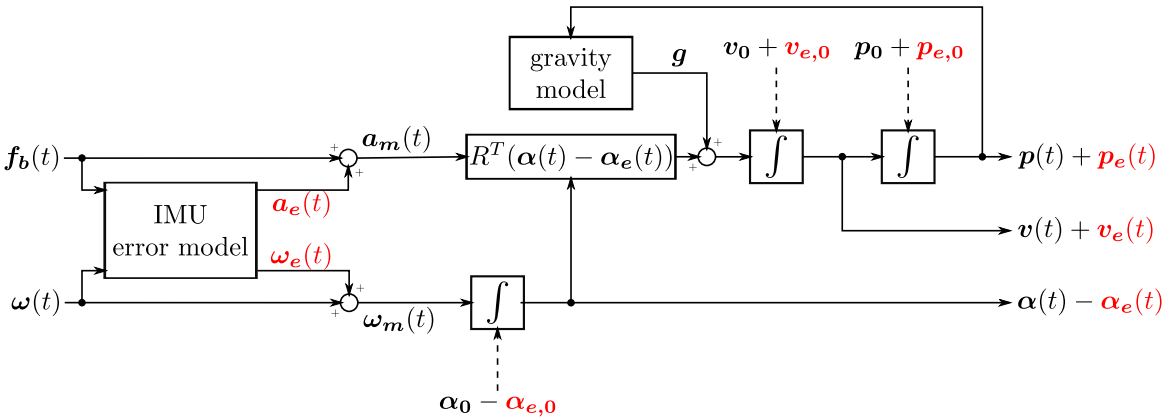

Figure 2 – Block diagram of basic strap-down INS signals propagation for accuracy analysis

$R(\boldsymbol{\alpha}(t)) = \exp\left([\boldsymbol{\alpha}(t)]_\times\right)$ — Matrix of rotation from navigation coordinate system to body coordinate system;
$[\boldsymbol{\alpha}(t)]_\times$ — vector of rotation skew–symmetric matrix;
$\boldsymbol{f_b}(t) = \boldsymbol{a}(t) + \boldsymbol{\omega}(t) \times \boldsymbol{u}(t) - R(\boldsymbol{\alpha}(t))\boldsymbol{g}$ — specific force;
$\boldsymbol{u}(t)$ — velocity in body coordinate system;
$\boldsymbol{a}(t) = \dot{\boldsymbol{u}}(t)$ — body acceleration, expressed in body coordinate system;
$\boldsymbol{\omega}(t)$ — body angular rate expressed in body coordinate system;
$\boldsymbol{g}$ — vector of gravity;
$\boldsymbol{\omega_e}(t)$, $\boldsymbol{a_e}(t)$ — vectors of angular rate and acceleration measurement error.
Symbols with subscript 0 denote initial values.

2.1 Error propagation model

For the considered navigation system shown in Figure 2, having made the following assumptions:

1. the navigation system is orthogonal and inertial (flat earth approximation);
2. orientation errors during navigation are small;
3. error products are ignored;

the following error propagation model can be determined [13]

$$\dot{\boldsymbol{\alpha}}_{\boldsymbol{e}}(t) = R^T(\boldsymbol{\alpha}(t))\,\boldsymbol{\omega_e}(t) \tag{3}$$

$$\dot{\boldsymbol{v}}_{\boldsymbol{e}}(t) = \boldsymbol{\alpha_e}(t) \times \boldsymbol{f_n}(t) + R^T(\boldsymbol{\alpha}(t))\,\boldsymbol{a_e}(t) \tag{4}$$

$$\dot{\boldsymbol{p}}_{\boldsymbol{e}}(t) = \boldsymbol{v_e}(t) \tag{5}$$

From the above model of the navigation system, and the error propagation model, the general formulas, equations (6) and (7) , for the orientation and position determination error are derived, which are difficult to solve in the general case for the whole trajectory, and a typical approach would be a numerical simulation.

$$\boldsymbol{\alpha_e}(t) = \boldsymbol{\alpha}_{e,0} + \int_0^t R^T(\boldsymbol{\alpha}(t))\left(\boldsymbol{\omega_b} + (S_\omega M_\omega - I)\,\boldsymbol{\omega}(t)\right)\mathrm{d}t + \int_0^t R^T(\boldsymbol{\alpha}(t))\,\Omega_g M_\omega\,\boldsymbol{f_b}(t)\,\mathrm{d}t \tag{6}$$

$$\boldsymbol{p_e}(t) = \boldsymbol{p}_{0,e} + t\,\boldsymbol{v}_{0,e} + \int_0^t \int_0^t \boldsymbol{\alpha_e}(t) \times R^T(\boldsymbol{\alpha}(t))\,\boldsymbol{f_b}(t)\,\mathrm{d}t\,\mathrm{d}t + \int_0^t \int_0^t R^T(\boldsymbol{\alpha}(t))\left(\boldsymbol{a_b} + (S_a M_a - I)\,\boldsymbol{f_b}(t)\right)\mathrm{d}t\,\mathrm{d}t \tag{7}$$

3. Methodology and considered cases

However, solution of the equations (6) and (7) can be done quite easily, after assuming piecewise constant motion characteristics, according to equations (8) to (11).

$$\boldsymbol{a}(t) = \boldsymbol{a} = \text{const} \tag{8}$$
$$\boldsymbol{\omega}(t) = \boldsymbol{\omega} = \text{const} \tag{9}$$
$$\boldsymbol{u}(t) = \boldsymbol{u_0} + \boldsymbol{a}t \tag{10}$$
$$R(\boldsymbol{\alpha}(t)) = \exp(-\Omega t)\, R(\boldsymbol{\alpha_0}) \tag{11}$$

where
$\Omega = [\omega]_\times$ — angular rate skew–symmetric matrix.
The symbolic solution is still a complicated task for human, however, it can be done easily with the help of symbolic computing software. In the case of this paper, Matlab with Symbolic Math Toolbox was used. Nevertheless, still the results obtained turn out to be very extensive. Thus, to facilitate the reader's understanding of the results presented, the analysis does not consider the whole assumed trajectory, but decomposes it into individual stages, considering each maneuver separately, and analyzing changes in the obtained error equations. The cases considered are summarized in Table 1.

Table 1 – List of considered maneuvers

No. case	α_0	ω	v_0	a	Eq. α_e	Eq. p_e	motion description
1	$\mathbf{0}$	$\mathbf{0}$	$\mathbf{0}$	$\boldsymbol{g}$	(16)	(24)	free fall
2	$\boldsymbol{\alpha_0}$	$\mathbf{0}$	$\mathbf{0}$	$\boldsymbol{g}$	(17)	(25)	free fall in arbitrary orientation
3	$\mathbf{0}$	$\mathbf{0}$	$\mathbf{0}$	$\mathbf{0}$	(18)	(26)	rest
4	$\boldsymbol{\alpha_0}$	$\mathbf{0}$	$\mathbf{0}$	$\mathbf{0}$	(19)	(27)	rest in arbitrary orientation
5	$\boldsymbol{\alpha_0}$	$\mathbf{0}$	$\boldsymbol{v_0}$	$\mathbf{0}$	(19)	(27)	steady rectilinear motion
6	$\mathbf{0}$	$\begin{bmatrix}0\\0\\w_z\end{bmatrix}$	$\mathbf{0}$	$\boldsymbol{g}$, $\dot{\boldsymbol{u}} = \mathbf{0}$	(20)	(28)	free fall with rotation
7	$\mathbf{0}$	$\begin{bmatrix}0\\0\\w_z\end{bmatrix}$	$\mathbf{0}$	$\mathbf{0}$	(21)	(29)	rotation without translation
8	$\mathbf{0}$	$\begin{bmatrix}0\\0\\w_z\end{bmatrix}$	$\begin{bmatrix}v_{0,x}\\0\\0\end{bmatrix}$	$\mathbf{0}$	(22)	(30)	circular motion
9	$\mathbf{0}$	$\begin{bmatrix}0\\0\\w_z\end{bmatrix}$	$\begin{bmatrix}v_{0,x}\\0\\0\end{bmatrix}$	$\begin{bmatrix}a_{sx}\\0\\0\end{bmatrix}$	(23)	(31)	spiral motion

In order to maintain the detail of the presented results and direct insight into the emerging dependencies, the individual components of the vectors were decomposed. However, for this to be possible, a detailed model of the measurement system had to be adopted by specifying the exact structure of the sensor model matrices.

3.1 Detailed measurement system model

Based on a review of the documentation of commercially available sensors, it is possible to distinguish the parameters that are given in almost every specification, so their use in the model will allow a direct comparison of IMU capabilities by substituting the parameters of their sensors into the formulas obtained from the analysis. The parameters thus selected are summarized in Table 2. It should be noted that listed parameters are typical for IMUs available on the market, which represent only a cross-section of existing sensor technologies. Therefore, it should be assumed that models presented below, based on these parameters, are applicable to optical gyroscopes (RLG, FOG) and sensors manufactured with MEMS technology.
Since in the considered measuring system triads of sensors are used, while in the specification only one value of each parameter is given, identical errors of each sensor in the triad were assumed. It was also assumed that gyroscopes and accelerometers have the same error matrix structures. The

adopted matrices are shown in equations (12) to (14).

$$S_i = \begin{bmatrix} 1+\varepsilon_i & 0 & 0 \\ 0 & 1+\varepsilon_i & 0 \\ 0 & 0 & 1+\varepsilon_i \end{bmatrix} \tag{12}$$

$$M_i = \begin{bmatrix} \sqrt{1-\delta_i^2} & \delta_i/\sqrt{2} & \delta_i/\sqrt{2} \\ \delta_i/\sqrt{2} & \sqrt{1-\delta_i^2} & \delta_i/\sqrt{2} \\ \delta_i/\sqrt{2} & \delta_i/\sqrt{2} & \sqrt{1-\delta_i^2} \end{bmatrix} \tag{13}$$

$$\Omega_g = \begin{bmatrix} \omega_g & 0 & 0 \\ 0 & \omega_g & 0 \\ 0 & 0 & \omega_g \end{bmatrix} \tag{14}$$

where index i should be replaced by a for accelerometers or ω for gyroscopes, while $\delta_i = \sin(\alpha_i)$, and α_i is sensor input axis misalignment [3].

3.2 Notes on analysis

In the analysis of the cases where rotation occurs, sensor measurement errors due to measurement noise have been omitted. The analysis of the impact of stochastic errors in a rotating navigation system is addressed, e.g., in [11].

It is assumed that the object makes 'coordinated' turns, that is, an object moving at speed $\boldsymbol{u} \neq \boldsymbol{0}$ cannot change orientation without changing direction of motion (except in the case of rotation along the direction of motion), and the resulting centripetal acceleration is equal $\boldsymbol{\omega} \times \boldsymbol{u}$. This assumption follows from the practical consideration that most objects move in a particular direction – 'forward'. The exception is the case with free fall, for which considered is motion with velocity $\boldsymbol{u} \approx \boldsymbol{0}$ or in orbit, where the constraint may not hold.

In the analysis, the error of the initial velocity is expressed in the navigation coordinate system. However, if the initial velocity in the coordinate system is determined by the velocity expressed in the body system and the orientation of the body, the initial velocity error results from the velocity errors in

Table 2 – Sensors parameters specified in almost all of IMU datasheets

Symbol	Parameter	Units
	Gyroscopes	
—	Input range	$^\circ/\mathrm{s}$
ω_b	Bias instability	$^\circ/\mathrm{s}$ or $^\circ/\mathrm{h}$
ε_ω	Scale factor accuracy	% or ppm
ARW	Angle Random Walk	$^\circ/\sqrt{\mathrm{h}}$
—	Noise density	$(^\circ/\mathrm{s})/\sqrt{\mathrm{Hz}}$
α_ω	Input axis misalignment	$^\circ$ or mrad
—	Bandwidth	Hz
ω_g	bias acceleration sensitivity	$(^\circ/\mathrm{s})/g$
	Accelerometers	
—	Input range	g
a_b	Bias instability	mg
ε_a	Scale factor accuracy	% or ppm
VRW	Velocity Random Walk	$(\mathrm{m/s})/\sqrt{\mathrm{h}}$
—	Noise density	$\mathrm{mg}/\sqrt{\mathrm{Hz}}$
α_a	Input axis misalignment	$^\circ$ or mrad
—	Bandwidth	Hz

the body system and the orientation error, as in equation (15).

$$\boldsymbol{v}_{e,0} = \boldsymbol{\alpha}_{e,0} \times \boldsymbol{v_0} + R^T(\boldsymbol{\alpha_0})\,\boldsymbol{u}_{e,0} \tag{15}$$

4. Analysis of results

The analysis of the obtained results will begin with the simplest case, and we will gradually move through the more complicated ones, adding successively the individual motion parameters. We will begin by analyzing the error of orientation determination, as the error obtained will be used further to determine the position error.

The first two cases is free fall, with the body coordinate system aligned to the navigation coordinate system and in arbitrary orientation. As can be seen in equations (16) and (17), consists of only initial and time dependent errors (bias and random walk).

$$\boldsymbol{\alpha_e}(t) = \begin{bmatrix} \alpha_{e,0,x} \\ \alpha_{e,0,y} \\ \alpha_{e,0,z} \end{bmatrix} + \begin{bmatrix} \omega_{b,x}t + \mathrm{arw}\sqrt{t} \\ \omega_{b,y}t + \mathrm{arw}\sqrt{t} \\ \omega_{b,z}t + \mathrm{arw}\sqrt{t} \end{bmatrix} \tag{16}$$

$$\boldsymbol{\alpha_e}(t) = \begin{bmatrix} \alpha_{e,0,x} \\ \alpha_{e,0,y} \\ \alpha_{e,0,z} \end{bmatrix} + R^T(\boldsymbol{\alpha_0}) \begin{bmatrix} \omega_{b,x}t + \mathrm{arw}\sqrt{t} \\ \omega_{b,y}t + \mathrm{arw}\sqrt{t} \\ \omega_{b,z}t + \mathrm{arw}\sqrt{t} \end{bmatrix} \tag{17}$$

If we place the system stationary, as in case 3 shown in equation (18), there is an error due to the acceleration sensitivity of the gyroscopes. Generalizing to arbitrary orientation in case 4, presented in equation (19), the only results is error rotation. Due to the change in the basis of the g-sensitivity matrix and the appearance of multiple trigonometric functions, the gravitational acceleration dependent term is not expanded and is written in the general, matrix, form. In the case shown, the acceleration is the ground reaction against the gravitational force, but an identical term will appear for any acceleration $\boldsymbol{a}(t)$. It is interesting to note, however, that identical results to those presented by the equation (19) will also be obtained for case 5, that is, when the object is moving in steady rectilinear motion, in arbitrary direction with arbitrary speed and orientation. This means that, from the point of view of the orientation error, it does not matter whether the body is at rest or moves with constant velocity. And hence, in the case of steady motion, an analysis that only takes into account time-dependent errors is perfectly sufficient.

$$\boldsymbol{\alpha_e}(t) = \begin{bmatrix} \alpha_{e,0,x} \\ \alpha_{e,0,y} \\ \alpha_{e,0,z} \end{bmatrix} + \begin{bmatrix} \omega_{b,x}t + \mathrm{arw}\sqrt{t} \\ \omega_{b,y}t + \mathrm{arw}\sqrt{t} \\ \omega_{b,z}t + \mathrm{arw}\sqrt{t} \end{bmatrix} + \omega_g t \begin{bmatrix} -\frac{1}{\sqrt{2}}\,\delta_w \\ -\frac{1}{\sqrt{2}}\,\delta_w \\ -\sqrt{1-{\delta_w}^2} \end{bmatrix} g_0 \tag{18}$$

$$\boldsymbol{\alpha_e}(t) = \begin{bmatrix} \alpha_{e,0,x} \\ \alpha_{e,0,y} \\ \alpha_{e,0,z} \end{bmatrix} + R^T(\boldsymbol{\alpha_0}) \begin{bmatrix} \omega_{b,x}t + \mathrm{arw}\sqrt{t} \\ \omega_{b,y}t + \mathrm{arw}\sqrt{t} \\ \omega_{b,z}t + \mathrm{arw}\sqrt{t} \end{bmatrix} + t\,R^T(\boldsymbol{\alpha_0})\,\Omega_g\,M_\omega\,R(\boldsymbol{\alpha_0})\,(-\boldsymbol{g}) \tag{19}$$

The next cases present formulas for the error of orientation determination, for motion containing rotations.

Case 6, shown in equation (20), represents free fall, similar to that shown in equation (16), but with rotation around Z axis. Comparing the two equations, one can see that the errors depend on time (only bias in this case), as well as gyroscope misalignment and scale factor errors. Most significantly, however, the errors in axes perpendicular to the rotation vector no longer increase linearly with time, but have a limited maximum value. This implies a significant reduction of the attitude errors and analytically demonstrate the correctness of results from the publications [1] and [8]. Moreover, it extends the results from the aforementioned publications, since, as can be seen from the formulas (21) and (22), for cases 7 and 8, the identical effect as for the gyroscope bias also occurs for g–sensitive errors emerging from gravitational and centripetal acceleration during circular motion.

$$\boldsymbol{\alpha_e}(t) = \begin{bmatrix} \alpha_{e,0,x} \\ \alpha_{e,0,y} \\ \alpha_{e,0,z} \end{bmatrix} + \begin{bmatrix} \left(\frac{\omega_{b,x}}{w_z} + \frac{1}{\sqrt{2}}\,\delta_w\,(\varepsilon_w+1)\right)\sin(t\,w_z) + \left(-\frac{2\,\omega_{b,y}}{w_z} - \sqrt{2}\,\delta_w\,(\varepsilon_w+1)\right)\sin\left(\frac{t\,w_z}{2}\right)^2 \\ \left(\frac{\omega_{b,y}}{w_z} + \frac{1}{\sqrt{2}}\,\delta_w\,(\varepsilon_w+1)\right)\sin(t\,w_z) + \left(\frac{2\,\omega_{b,x}}{w_z} + \sqrt{2}\,\delta_w\,(\varepsilon_w+1)\right)\sin\left(\frac{t\,w_z}{2}\right)^2 \\ \left(\omega_{b,z} - w_z\left(1-(\varepsilon_a+1)\sqrt{1-{\delta_a}^2}\right)\right)t \end{bmatrix} \tag{20}$$

$$= \begin{bmatrix} \alpha_{e,0,x} \\ \alpha_{e,0,y} \\ \alpha_{e,0,z} \end{bmatrix} + R^T(\boldsymbol{\alpha_0}) \int_0^t \exp(\Omega t)\,\mathrm{d}t\,(\boldsymbol{\omega_b} + (S_\omega M_\omega - I)\,\boldsymbol{\omega})$$

$$\boldsymbol{\alpha_e}(t) = \begin{bmatrix} \alpha_{e,0,x} \\ \alpha_{e,0,y} \\ \alpha_{e,0,z} \end{bmatrix} + \begin{bmatrix} \left(\frac{\omega_{b,x}}{w_z} + \frac{1}{\sqrt{2}}\,\delta_w\,(\varepsilon_w+1)\right)\sin(t\,w_z) + \left(-\frac{2\,\omega_{b,y}}{w_z} - \sqrt{2}\,\delta_w\,(\varepsilon_w+1)\right)\sin\left(\frac{t\,w_z}{2}\right)^2 \\ \left(\frac{\omega_{b,y}}{w_z} + \frac{1}{\sqrt{2}}\,\delta_w\,(\varepsilon_w+1)\right)\sin(t\,w_z) + \left(\frac{2\,\omega_{b,x}}{w_z} + \sqrt{2}\,\delta_w\,(\varepsilon_w+1)\right)\sin\left(\frac{t\,w_z}{2}\right)^2 \\ \left(\omega_{b,z} - w_z\left(1-(\varepsilon_a+1)\sqrt{1-{\delta_a}^2}\right)\right)t \end{bmatrix}$$
$$+ \omega_g \begin{bmatrix} -\frac{\sqrt{2}\,\delta_w\sin(t\,w_z)}{2\,w_z} + \frac{\sqrt{2}\,\delta_w\sin\left(\frac{t\,w_z}{2}\right)^2}{w_z} \\ -\frac{\sqrt{2}\,\delta_w\sin(t\,w_z)}{2\,w_z} - \frac{\sqrt{2}\,\delta_w\sin\left(\frac{t\,w_z}{2}\right)^2}{w_z} \\ -t\sqrt{1-{\delta_w}^2} \end{bmatrix} g_0 \tag{21}$$

$$= \begin{bmatrix} \alpha_{e,0,x} \\ \alpha_{e,0,y} \\ \alpha_{e,0,z} \end{bmatrix} + R^T(\boldsymbol{\alpha_0}) \int_0^t \exp(\Omega t)\,\mathrm{d}t\,(\boldsymbol{\omega_b} + (S_\omega M_\omega - I)\,\boldsymbol{\omega})$$
$$+ R^T(\boldsymbol{\alpha_0}) \int_0^t \exp(\Omega t)\,\Omega_g M_\omega \exp(-\Omega t)\,\mathrm{d}t\,R(\boldsymbol{\alpha_0})\,(-\boldsymbol{g})$$

$$\boldsymbol{\alpha_e}(t) = \begin{bmatrix} \alpha_{e,0,x} \\ \alpha_{e,0,y} \\ \alpha_{e,0,z} \end{bmatrix} + \begin{bmatrix} \left(\frac{\omega_{b,x}}{w_z} + \frac{1}{\sqrt{2}}\,\delta_w\,(\varepsilon_w+1)\right)\sin(t\,w_z) + \left(-\frac{2\,\omega_{b,y}}{w_z} - \sqrt{2}\,\delta_w\,(\varepsilon_w+1)\right)\sin\left(\frac{t\,w_z}{2}\right)^2 \\ \left(\frac{\omega_{b,y}}{w_z} + \frac{1}{\sqrt{2}}\,\delta_w\,(\varepsilon_w+1)\right)\sin(t\,w_z) + \left(\frac{2\,\omega_{b,x}}{w_z} + \sqrt{2}\,\delta_w\,(\varepsilon_w+1)\right)\sin\left(\frac{t\,w_z}{2}\right)^2 \\ \left(\omega_{b,z} - w_z\left(1-(\varepsilon_a+1)\sqrt{1-{\delta_a}^2}\right)\right)t \end{bmatrix}$$
$$+ \omega_g \begin{bmatrix} -\frac{\sqrt{2}\,\delta_w\sin(t\,w_z)}{2\,w_z} + \frac{\sqrt{2}\,\delta_w\sin\left(\frac{t\,w_z}{2}\right)^2}{w_z} \\ -\frac{\sqrt{2}\,\delta_w\sin(t\,w_z)}{2\,w_z} - \frac{\sqrt{2}\,\delta_w\sin\left(\frac{t\,w_z}{2}\right)^2}{w_z} \\ -\sqrt{1-{\delta_w}^2} \end{bmatrix} g_0 + \omega_g \begin{bmatrix} \frac{1}{\sqrt{2}}\,\delta_w\sin(t\,w_z) - 2\sin\left(\frac{t\,w_z}{2}\right)^2\sqrt{1-{\delta_w}^2} \\ \sin(t\,w_z)\sqrt{1-{\delta_w}^2} + \sqrt{2}\,\delta_w\sin\left(\frac{t\,w_z}{2}\right)^2 \\ +\frac{1}{\sqrt{2}}\,\delta_w\,t\,w_z \end{bmatrix} u_{0,x} \tag{22}$$

$$= \begin{bmatrix} \alpha_{e,0,x} \\ \alpha_{e,0,y} \\ \alpha_{e,0,z} \end{bmatrix} + R^T(\boldsymbol{\alpha_0}) \int_0^t \exp(\Omega t)\,\mathrm{d}t\,(\boldsymbol{\omega_b} + (S_\omega M_\omega - I)\,\boldsymbol{\omega})$$
$$+ R^T(\boldsymbol{\alpha_0}) \int_0^t \exp(\Omega t)\,\Omega_g M_\omega \exp(-\Omega t)\,\mathrm{d}t\,R(\boldsymbol{\alpha_0})\,(-\boldsymbol{g}) + R^T(\boldsymbol{\alpha_0}) \int_0^t \exp(\Omega t)\,\mathrm{d}t\,\Omega_g M_\omega\,(\boldsymbol{\omega} \times \boldsymbol{u_0})$$

It is only the addition of constant acceleration in case 9, shown in equation (23) that causes the orientation error to increase linearly over time.

$$
\begin{aligned}
\boldsymbol{\alpha_e}(t) = &\begin{bmatrix}\alpha_{e,0,x}\\ \alpha_{e,0,y}\\ \alpha_{e,0,z}\end{bmatrix} + \begin{bmatrix}\left(\frac{\omega_{b,x}}{w_z} + \frac{1}{\sqrt{2}}\,\delta_w\,(\varepsilon_w+1)\right)\sin(t\,w_z) + \left(-\frac{2\,\omega_{b,y}}{w_z} - \sqrt{2}\,\delta_w\,(\varepsilon_w+1)\right)\sin\left(\frac{t\,w_z}{2}\right)^2\\ \left(\frac{\omega_{b,y}}{w_z} + \frac{1}{\sqrt{2}}\,\delta_w\,(\varepsilon_w+1)\right)\sin(t\,w_z) + \left(\frac{2\,\omega_{b,x}}{w_z} + \sqrt{2}\,\delta_w\,(\varepsilon_w+1)\right)\sin\left(\frac{t\,w_z}{2}\right)^2\\ \left(\omega_{b,z} - w_z\left(1-(\varepsilon_a+1)\sqrt{1-{\delta_a}^2}\right)\right)t\end{bmatrix}\\
&+\omega_g\begin{bmatrix}-\frac{\sqrt{2}\,\delta_w\sin(t\,w_z)}{2\,w_z} + \frac{\sqrt{2}\,\delta_w\sin\left(\frac{t\,w_z}{2}\right)^2}{w_z}\\ -\frac{\sqrt{2}\,\delta_w\sin(t\,w_z)}{2\,w_z} - \frac{\sqrt{2}\,\delta_w\sin\left(\frac{t\,w_z}{2}\right)^2}{w_z}\\ -t\sqrt{1-{\delta_w}^2}\end{bmatrix} g_0 + \omega_g\begin{bmatrix}\frac{1}{\sqrt{2}}\,\delta_w\,\sin(t\,w_z) - 2\sin\left(\frac{t\,w_z}{2}\right)^2\sqrt{1-{\delta_w}^2}\\ \sin(t\,w_z)\,\sqrt{1-{\delta_w}^2} + \sqrt{2}\,\delta_w\sin\left(\frac{t\,w_z}{2}\right)^2\\ \frac{1}{\sqrt{2}}\,\delta_w\,w_z\,t\end{bmatrix} u_{0,x}\\
&+\omega_g\begin{bmatrix}t\sqrt{1-{\delta_w}^2} - \frac{2\sqrt{2}\,\delta_w\sin\left(\frac{t\,w_z}{2}\right)^2}{w_z}\\ -\frac{1}{\sqrt{2}}\,\delta_w\,t + \frac{\sqrt{2}\,\delta_w\sin(t\,w_z)}{w_z}\\ \frac{1}{\sqrt{2}}\,\delta_w\,t\end{bmatrix} a_{\mathrm{sx}} + \omega_g\begin{bmatrix}\frac{1}{\sqrt{2}}\,\delta_w\,t\,\sin(t\,w_z) - 2\,t\sin\left(\frac{t\,w_z}{2}\right)^2\sqrt{1-{\delta_w}^2}\\ t\,\sin(t\,w_z)\,\sqrt{1-{\delta_w}^2} + \sqrt{2}\,\delta_w\,t\sin\left(\frac{t\,w_z}{2}\right)^2\\ \frac{1}{2\sqrt{2}}\,\delta_w\,w_z\,t^2\end{bmatrix} a_{\mathrm{sx}}\\
&= \begin{bmatrix}\alpha_{e,0,x}\\ \alpha_{e,0,y}\\ \alpha_{e,0,z}\end{bmatrix} + R^T(\boldsymbol{\alpha_0})\int_0^t \exp(\Omega t)\,\mathrm{d}t\,\left(\boldsymbol{\omega_b} + (S_\omega M_\omega - I)\,\boldsymbol{\omega}\right)\\
&+R^T(\boldsymbol{\alpha_0})\int_0^t \exp(\Omega t)\,\Omega_g\,M_\omega\,\exp(-\Omega t)\,\mathrm{d}t\,R(\boldsymbol{\alpha_0})\,(-\boldsymbol{g})\\
&+R^T(\boldsymbol{\alpha_0})\int_0^t \exp(\Omega t)\,t\,\mathrm{d}t\,\Omega_g\,M_\omega\,(\boldsymbol{\omega}\times\boldsymbol{a}) + R^T(\boldsymbol{\alpha_0})\int_0^t \exp(\Omega t)\,\mathrm{d}t\,\Omega_g\,M_\omega\,(\boldsymbol{\omega}\times\boldsymbol{u_0}+\boldsymbol{a})
\end{aligned}
\tag{23}
$$

However, rotation of the navigation system does not affect the orientation error in the axis parallel to the rotation vector. Moreover, continuous rotation causes an increase in the error of orientation determination in this axis due to the linearly increasing scale factor error.

The presented formulas assume velocity and acceleration in the X axis of the body coordinate system and rotation about the Z axis of the body coordinate system. However, the presented effects are satisfied for any cases of rotation. The observed effects will occur just on a different plane. To cover other cases, more general, matrix formulas are also presented for equations (20) to (23).

In the following part, we will again pass through all the considered maneuvers, this time analyzing the position determination error.

Analyzing cases 1 and 2 again, this time in terms of the position determination error, shown in the equations (24) and (25), one can find a similar relationship as for the orientation errors from equations (16) and (17) – the error depends only on the initial orientation errors and the time-dependent errors (bias and random walk). It can also be seen that as long as the specific force is equal to zero, the orientation and position errors are independent of each other (assuming the initial velocity error does not depend on the orientation errors)

$$
\boldsymbol{p_e}(t) = \begin{bmatrix}p_{e,0,x} + t\,v_{e,0,x}\\ p_{e,0,y} + t\,v_{e,0,y}\\ p_{e,0,z} + t\,v_{e,0,z}\end{bmatrix} + \begin{bmatrix}\frac{1}{2}\,a_{b,x}\,t^2 + \frac{2}{3}\,\mathrm{vrw}\,t^{3/2}\\ \frac{1}{2}\,a_{b,y}\,t^2 + \frac{2}{3}\,\mathrm{vrw}\,t^{3/2}\\ \frac{1}{2}\,a_{b,z}\,t^2 + \frac{2}{3}\,\mathrm{vrw}\,t^{3/2}\end{bmatrix} \tag{24}
$$

$$
\boldsymbol{p_e}(t) = \begin{bmatrix}p_{e,0,x} + t\,v_{e,0,x}\\ p_{e,0,y} + t\,v_{e,0,y}\\ p_{e,0,z} + t\,v_{e,0,z}\end{bmatrix} + R^T(\boldsymbol{\alpha_0})\begin{bmatrix}\frac{1}{2}\,a_{b,x}\,t^2 + \frac{2}{3}\,\mathrm{vrw}\,t^{3/2}\\ \frac{1}{2}\,a_{b,y}\,t^2 + \frac{2}{3}\,\mathrm{vrw}\,t^{3/2}\\ \frac{1}{2}\,a_{b,z}\,t^2 + \frac{2}{3}\,\mathrm{vrw}\,t^{3/2}\end{bmatrix} \tag{25}
$$

Only for cases 3 and 4, shown in equations(26) and (27), does the position determination error includes the misalignment and scale factor errors of accelerometers and incorporates the effect of orientation error on the position determination error. Leaving aside the scale and misalignment errors of accelerometers, this is the case that is typically used to determine the accuracy of a navigation system based on navigation duration.

Due to the increasing complexity of the relationships for case 4, some errors in equation (27) are presented in a general, matrix, form. For case number 5, similar to the orientation determination

error, the position determination error does not depend on the direction and velocity of the object motion and the errors equation is identical to case 4, presented in equation (27).

$$\begin{aligned}\boldsymbol{p_e}(t) = &\begin{bmatrix} p_{e,0,x} + t\,v_{e,0,x} \\ p_{e,0,y} + t\,v_{e,0,y} \\ p_{e,0,z} + t\,v_{e,0,z} \end{bmatrix} + \begin{bmatrix} \frac{1}{2}\,a_{b,x}\,t^2 + \frac{2}{3}\,\mathrm{vrw}\,t^{3/2} \\ \frac{1}{2}\,a_{b,y}\,t^2 + \frac{2}{3}\,\mathrm{vrw}\,t^{3/2} \\ \frac{1}{2}\,a_{b,z}\,t^2 + \frac{2}{3}\,\mathrm{vrw}\,t^{3/2} \end{bmatrix} + \frac{1}{2}\,t^2 \begin{bmatrix} -\frac{1}{\sqrt{2}}\,\delta_a\,(\varepsilon_a+1) \\ -\frac{1}{\sqrt{2}}\,\delta_a\,(\varepsilon_a+1) \\ 1-\sqrt{1-{\delta_a}^2}\,(\varepsilon_a+1) \end{bmatrix} g_0 \\ &+ \begin{bmatrix} -\frac{1}{2}\,\alpha_{e,0,y}\,t^2 - \frac{1}{6}\,\omega_{b,y}\,t^3 - \frac{4}{15}\,\mathrm{arw}\,t^{5/2} + \frac{\sqrt{2}}{12}\,\delta_w\,\omega_g\,g_0\,t^3 \\ \frac{1}{2}\,\alpha_{e,0,x}\,t^2 + \frac{1}{6}\,\omega_{b,x}\,t^3 + \frac{4}{15}\,\mathrm{arw}\,t^{5/2} - \frac{\sqrt{2}}{12}\,\delta_w\,\omega_g\,g_0\,t^3 \\ 0 \end{bmatrix} g_0 \end{aligned} \tag{26}$$

$$\begin{aligned}\boldsymbol{p_e}(t) = &\begin{bmatrix} p_{e,0,x} + t\,v_{e,0,x} \\ p_{e,0,y} + t\,v_{e,0,y} \\ p_{e,0,z} + t\,v_{e,0,z} \end{bmatrix} + R^T(\boldsymbol{\alpha_0}) \begin{bmatrix} \frac{1}{2}\,a_{b,x}\,t^2 + \frac{2}{3}\,\mathrm{vrw}\,t^{3/2} \\ \frac{1}{2}\,a_{b,y}\,t^2 + \frac{2}{3}\,\mathrm{vrw}\,t^{3/2} \\ \frac{1}{2}\,a_{b,z}\,t^2 + \frac{2}{3}\,\mathrm{vrw}\,t^{3/2} \end{bmatrix} + \frac{1}{2}\,t^2\,R^T(\boldsymbol{\alpha_0})\,(S_a M_a - I)\,R(\boldsymbol{\alpha_0})\,(-\mathbf{g}) \\ &+ \left(\frac{1}{2}\,t^2 \begin{bmatrix} \alpha_{e,0,x} \\ \alpha_{e,0,y} \\ \alpha_{e,0,z} \end{bmatrix} + R^T(\boldsymbol{\alpha_0}) \left(\frac{1}{6}\,t^3 \begin{bmatrix} \omega_{b,x} \\ \omega_{b,y} \\ \omega_{b,z} \end{bmatrix} + \frac{4}{15}\,t^{5/2} \begin{bmatrix} \mathrm{arw} \\ \mathrm{arw} \\ \mathrm{arw} \end{bmatrix} + \frac{1}{6}\,t^3\,\omega_g\,M_\omega\,R(\boldsymbol{\alpha_0})\,(-\mathbf{g}) \right) \right) \times (-\mathbf{g}) \\ = &\begin{bmatrix} p_{e,0,x} + t\,v_{e,0,x} \\ p_{e,0,y} + t\,v_{e,0,y} \\ p_{e,0,z} + t\,v_{e,0,z} \end{bmatrix} + R^T(\boldsymbol{\alpha_0}) \begin{bmatrix} \frac{1}{2}\,a_{b,x}\,t^2 + \frac{2}{3}\,\mathrm{vrw}\,t^{3/2} \\ \frac{1}{2}\,a_{b,y}\,t^2 + \frac{2}{3}\,\mathrm{vrw}\,t^{3/2} \\ \frac{1}{2}\,a_{b,z}\,t^2 + \frac{2}{3}\,\mathrm{vrw}\,t^{3/2} \end{bmatrix} + \frac{1}{2}\,t^2\,R^T(\boldsymbol{\alpha_0})\,(S_a M_a - I)\,R(\boldsymbol{\alpha_0})\,(-\mathbf{g}) \\ &+ \int_0^T \int_0^T \boldsymbol{\alpha_e(t)} \times (-\mathbf{g})\,\mathrm{d}t\,\mathrm{d}t \end{aligned} \tag{27}$$

Comparing case 6 from equation (28) to case 1 from equation (24), and case 7 from equation (29) to case 3 from equation (26), it can be seen that, also in the case of position determination error, rotation of navigation system allows the error dependence on time to be reduced from a quadratic to a linear dependence. the position error resulting from the orientation error in equation will be similar to that for (27). However, due to the more complicated formula for orientation error (from equation (21)), this component will not be expanded.

$$\begin{aligned}\boldsymbol{p_e}(t) = &\begin{bmatrix} p_{e,0,x} + t\,v_{e,0,x} \\ p_{e,0,y} + t\,v_{e,0,y} \\ p_{e,0,z} + t\,v_{e,0,z} \end{bmatrix} + \begin{bmatrix} -a_{b,y} \left(\frac{t}{w_z} - \frac{\sin(t\,w_z)}{{w_z}^2} \right) + 2\,a_{b,x}\,\frac{\sin\left(\frac{t\,w_z}{2}\right)^2}{{w_z}^2} \\ a_{b,x} \left(\frac{t}{w_z} - \frac{\sin(t\,w_z)}{{w_z}^2} \right) + 2\,a_{b,y}\,\frac{\sin\left(\frac{t\,w_z}{2}\right)^2}{{w_z}^2} \\ +\frac{1}{2}\,a_{b,z}\,t^2 \end{bmatrix} \\ = &\begin{bmatrix} p_{e,0,x} + t\,v_{e,0,x} \\ p_{e,0,y} + t\,v_{e,0,y} \\ p_{e,0,z} + t\,v_{e,0,z} \end{bmatrix} + R^T(\boldsymbol{\alpha_0}) \int_0^t \int_0^t \exp(\Omega t)\,\mathrm{d}t\,\mathrm{d}t\,\boldsymbol{a_b} \end{aligned} \tag{28}$$

$$\begin{aligned}\boldsymbol{p_e}(t) = &\begin{bmatrix} p_{e,0,x} + t\,v_{e,0,x} \\ p_{e,0,y} + t\,v_{e,0,y} \\ p_{e,0,z} + t\,v_{e,0,z} \end{bmatrix} + \begin{bmatrix} -a_{b,y} \left(\frac{t}{w_z} - \frac{\sin(t\,w_z)}{{w_z}^2} \right) + 2\,a_{b,x}\,\frac{\sin\left(\frac{t\,w_z}{2}\right)^2}{{w_z}^2} \\ a_{b,x} \left(\frac{t}{w_z} - \frac{\sin(t\,w_z)}{{w_z}^2} \right) + 2\,a_{b,y}\,\frac{\sin\left(\frac{t\,w_z}{2}\right)^2}{{w_z}^2} \\ \frac{1}{2}\,a_{b,z}\,t^2 \end{bmatrix} \\ &+ \begin{bmatrix} \frac{1}{\sqrt{2}}\,\delta_a\,(\varepsilon_a+1) \left(\frac{t}{w_z} - \frac{\sin(t\,w_z)}{w_z^2} \right) + -\sqrt{2}\,\delta_a\,(\varepsilon_a+1)\,\frac{\sin\left(\frac{t\,w_z}{2}\right)^2}{{w_z}^2} \\ -\frac{1}{\sqrt{2}}\,\delta_a\,(\varepsilon_a+1) \left(\frac{t}{w_z} - \frac{\sin(t\,w_z)}{w_z^2} \right) + -\sqrt{2}\,\delta_a\,(\varepsilon_a+1)\,\frac{\sin\left(\frac{t\,w_z}{2}\right)^2}{{w_z}^2} \\ \frac{1}{2} \left(1 - (\varepsilon_a+1)\,\sqrt{1-{\delta_a}^2} \right) t^2 \end{bmatrix} g_0 + \int_0^t \int_0^t \boldsymbol{\alpha_e}(t) \times (-\boldsymbol{g})\,\mathrm{d}t\,\mathrm{d}t \\ = &\begin{bmatrix} p_{e,0,x} + t\,v_{e,0,x} \\ p_{e,0,y} + t\,v_{e,0,y} \\ p_{e,0,z} + t\,v_{e,0,z} \end{bmatrix} + R^T(\boldsymbol{\alpha_0}) \int_0^t \int_0^t \exp(\Omega t)\,\mathrm{d}t\,\mathrm{d}t\,\boldsymbol{a_b} \\ &+ R^T(\boldsymbol{\alpha_0}) \int_0^t \int_0^t \exp(\Omega t)\,(S_a M_a - I)\,\exp(-\Omega t)\,\mathrm{d}t\,\mathrm{d}t\,R(\boldsymbol{\alpha_0})\,(-\boldsymbol{g}) + \int_0^t \int_0^t \boldsymbol{\alpha_e}(t) \times (-\boldsymbol{g})\,\mathrm{d}t\,\mathrm{d}t \end{aligned} \tag{29}$$

Result for case 8 in equation (30) relative to the case in equation (29) adds a component resulting from centripetal acceleration in circular motion. The last of the analyzed cases, presented in equation (31) turned out to be too complex to be presented in expanded form in the paper. Hence, only the general, matrix form is presented. However, it is the most general form, including all of motion parameters, and divided so that interpretation of the individual components is straightforward.

$$\begin{aligned}
\boldsymbol{p_e}(t) = &\begin{bmatrix} p_{e,0,x} + t\,v_{e,0,x} \\ p_{e,0,y} + t\,v_{e,0,y} \\ p_{e,0,z} + t\,v_{e,0,z} \end{bmatrix} + \begin{bmatrix} -a_{b,y}\left(\frac{t}{w_z} - \frac{\sin(t\,w_z)}{{w_z}^2}\right) + 2\,a_{b,x}\,\frac{\sin\left(\frac{t\,w_z}{2}\right)^2}{{w_z}^2} \\ a_{b,x}\left(\frac{t}{w_z} - \frac{\sin(t\,w_z)}{{w_z}^2}\right) + 2\,a_{b,y}\,\frac{\sin\left(\frac{t\,w_z}{2}\right)^2}{{w_z}^2} \\ \frac{1}{2}\,a_{b,z}\,t^2 \end{bmatrix} \\
&+ \begin{bmatrix} \frac{1}{\sqrt{2}}\,\delta_a\,(\varepsilon_a+1)\left(\frac{t}{w_z} - \frac{\sin(t\,w_z)}{w_z^2}\right) + -\sqrt{2}\,\delta_a\,(\varepsilon_a+1)\,\frac{\sin\left(\frac{t\,w_z}{2}\right)^2}{{w_z}^2} \\ -\frac{1}{\sqrt{2}}\,\delta_a\,(\varepsilon_a+1)\left(\frac{t}{w_z} - \frac{\sin(t\,w_z)}{w_z^2}\right) + -\sqrt{2}\,\delta_a\,(\varepsilon_a+1)\,\frac{\sin\left(\frac{t\,w_z}{2}\right)^2}{{w_z}^2} \\ \frac{1}{2}\left(1 - (\varepsilon_a+1)\sqrt{1-{\delta_a}^2}\right)t^2 \end{bmatrix} g_0 \\
&+ \begin{bmatrix} \left(1 - (\varepsilon_a+1)\sqrt{1-{\delta_a}^2}\right)\left(t - \frac{\sin(t\,w_z)}{w_z}\right) + \sqrt{2}\,\delta_a\,(\varepsilon_a+1)\,\frac{\sin\left(\frac{t\,w_z}{2}\right)^2}{w_z} \\ \frac{1}{\sqrt{2}}\,\delta_a\,(\varepsilon_a+1)\left(t - \frac{\sin(t\,w_z)}{w_z}\right) - 2\left(1 - (\varepsilon_a+1)\sqrt{1-{\delta_a}^2}\right)\frac{\sin\left(\frac{t\,w_z}{2}\right)^2}{w_z} \\ \frac{1}{2\sqrt{2}}\,\delta_a\,w_z\,(\varepsilon_a+1)\,t^2 \end{bmatrix} u_{0,x} \\
&+ \int_0^t\int_0^t \boldsymbol{\alpha_e}(t) \times \left(R^T(\boldsymbol{\alpha_0})\exp(\Omega t)\,(\boldsymbol{\omega}\times\boldsymbol{u_0}) - \boldsymbol{g}\right)\mathrm{d}t\,\mathrm{d}t
\end{aligned} \tag{30}$$

$$\begin{aligned}
\boldsymbol{p_e}(t) = &\,\boldsymbol{p}_{e,0} + t\,\boldsymbol{v}_{e,0} + R^T(\boldsymbol{\alpha_0})\int_0^t\int_0^t \exp(\Omega t)\,\mathrm{d}t\,\mathrm{d}t\,\boldsymbol{a_b} \\
&+ R^T(\boldsymbol{\alpha_0})\int_0^t\int_0^t \exp(\Omega t)\,(S_a M_a - I)\exp(-\Omega t)\,\mathrm{d}t\,\mathrm{d}t\,R(\boldsymbol{\alpha_0})\,(-\boldsymbol{g}) \\
&+ R^T(\boldsymbol{\alpha_0})\int_0^t\int_0^t \exp(\Omega t)\,\mathrm{d}t\,\mathrm{d}t\,(S_a M_a - I)\,(\boldsymbol{a} + \boldsymbol{\omega}\times\boldsymbol{u_0}) \\
&+ R^T(\boldsymbol{\alpha_0})\int_0^t\int_0^t \exp(\Omega t)\,t\,\mathrm{d}t\,\mathrm{d}t\,(S_a M_a - I)\,(\boldsymbol{\omega}\times\boldsymbol{a}) \\
&+ \int_0^t\int_0^t \boldsymbol{\alpha_e}(t) \times \left(R^T(\boldsymbol{\alpha_0})\exp(\Omega t)\,(\boldsymbol{a} + \boldsymbol{\omega}\times\boldsymbol{u_0} + \boldsymbol{\omega}\times\boldsymbol{a}\,t) - \boldsymbol{g}\right)\mathrm{d}t\,\mathrm{d}t
\end{aligned} \tag{31}$$

The conducted analysis shows that assuming piecewise values of motion parameters, each fragment of the trajectory can be analyzed separately. It is only necessary to assign appropriate initial conditions resulting from the preceding fragments. Moreover, the impact of each error within a single trajectory fragment can be analyzed separately.

The analyzed cases of maneuvers in which there was no rotation seem to be trivial. However, they made it possible to show the influence of the individual motion parameters and the parameters of the measurement system model on the resulting errors of orientation or position determination. The obtained results indicate that the errors accumulating during steady motion do not differ from the errors accumulating when the object is stationary, and depend only on time. This observation allows to conclude that it is sufficient to determine errors on the basis of navigation duration complemented with more detailed analysis only for fragments containing high dynamics of motion (significant accelerations, or changes of direction – especially the rapid ones).

The analysis of cases of maneuvers with rotation returns more interesting results. It can be seen that in many of the analyzed cases, the orientation or position error is the product of the appropriate integral of $\exp(\Omega(t))$ and a constant vector. Equation (32) presents the first integral of $\exp(\Omega(t))$ for rotation about the Z axis.

$$\int_0^t \exp(\Omega t)\,\mathrm{d}t = \begin{bmatrix} \frac{\sin(t\,w_z)}{w_z} & -\frac{2\sin\left(\frac{t\,w_z}{2}\right)^2}{w_z} & 0 \\ \frac{2\sin\left(\frac{t\,w_z}{2}\right)^2}{w_z} & \frac{\sin(t\,w_z)}{w_z} & 0 \\ 0 & 0 & t \end{bmatrix} \tag{32}$$

Already that allows to notice that continuous rotation allows to reduce the dependence of the error on time, in the plane perpendicular to the rotation axis, by reducing the exponent at variable t by 1.

5. Conclusions

The paper presents an analysis of the results of calculations of errors of orientation and position determination for an unaided strapdown inertial navigation system under the influence of various maneuvers. The method used allowed for the determination of analytical formulas, which made it possible to clearly observe and understand the existing dependencies. On the basis of the presented formulas, conclusions were drawn concerning the propagation of navigation errors both in the case of the occurrence of low and high dynamic motion. This will allow more accurate analysis of navigational systems and more precise specification of requirements for selecting measurement systems.

6. Contact Author Email Address

mailto: Krystian.Borodacz@ilot.lukasiewicz.gov.pl

7. Copyright Statement

References

[1] Ben Y yang, Chai Y li, Gao W, Sun F. Analysis of error for a rotating strap-down inertial navigation system with fibro gyro. *J Marine Sci Appl*, Vol. 9, No. 4, pp 419-424, 2010.

[2] Borodacz K, Szczepański C, Popowski S. Review and selection of commercially available IMU for a short time inertial navigation. *AEAT*, Vol. 94, No. 1, pp 45-59, 2022.

[3] IEEE Std 528-2019. *IEEE Standard for Inertial Sensor Terminology*. IEEE, 2019.

[4] IEEE Std 647-2006 *IEEE Standard Specification Format Guide and Test Procedure for Single-Axis Laser Gyros*. IEEE, 2006.

[5] IEEE Std 952-2020. *IEEE Standard for Specifying and Testing Single-Axis Interferometric Fiber Optic Gyros*. IEEE, 2020.

[6] IEEE Std 1293-2018. *IEEE Standard Specification Format Guide and Test Procedure for Linear Single-Axis, Nongyroscopic Accelerometers*. IEEE, 2018.

[7] IEEE Std 1559-2009. *IEEE Standard for Inertial Systems Terminology*. IEEE, 2009.

[8] Ishibashi S, Tsukioka S, Yoshida H, et al. Accuracy Improvement of an Inertial Navigation System Brought about by the Rotational Motion. *OCEANS 2007 - Europe*, pp 1-5, 2007.

[9] Lawrence A. *Modern Inertial Technology. Navigation, Guidance, and Control*. 2nd edition, Springer-Verlag, 1998.

[10] Li K, Gao P, Wang L, Zhang Q. Analysis and Improvement of Attitude Output Accuracy in Rotation Inertial Navigation System. *Mathematical Problems in Engineering*. pp 1-10, 2015.

[11] Lv P, Lai J, Liu J, Nie M. The Compensation Effects of Gyros' Stochastic Errors in a Rotational Inertial Navigation System. *J Navigation*, Vol. 67, No. 6, pp 1069-1088, 2014.

[12] Unsal D, Demirbas K. Estimation of deterministic and stochastic IMU error parameters. *Proceedings of the 2012 IEEE/ION Position, Location and Navigation Symposium*, Myrtle Beach, pp 862-868, 2012.

[13] Titterton D, Weston J. *Strapdown Inertial Navigation Technology*. 2nd edition, Institution of Electrical Engineers, 2004.